AIAA JOURNAL
Vol. 42, No. 3, March 2004

Helicopter Vibration Reduction Using Fixed-System Auxiliary Moments

Farhan Gandhi*
Pennsylvania State University, University Park, Pennsylvania 16802
and
Martin K. Sekula†
NASA Langley Research Center, Hampton, Virginia 23681

Reductions in helicopter rotor hub vibratory loads that can be obtained through the introduction of steady auxiliary pitching and rolling moments in the fixed system are examined. The auxiliary moments allow changes in vehicle attitude and rotor pitch control inputs, such that vibrations can be minimized, while vehicle equilibrium is still satisfied. Because auxiliary moments can be generated by variation of the pitch of the right and left halves of the horizontal tail, the weight penalty, complexity, and performance losses associated with auxiliary lift and thrust (conventional compounding) would be alleviated. A comprehensive rotorcraft aeroelastic analysis was modified to include the fixed system auxiliary moments in the trim equations, and vibration reductions were examined for two different cases: 1) a light BO-105 type helicopter with a four-bladed hingeless rotor at high flight speeds (advance ratio of 0.35) and 2) a medium-weight UH-60 type helicopter with a four-bladed articulated rotor at a more moderate flight speed (advance ratio of 0.25). For the BO-105 type aircraft, a nosedown auxiliary pitching moment and a roll-left auxiliary rolling moment could reduce the in-plane vibratory hub forces by 20–30% when used individually and by 90% when used in combination. For the UH-60 type aircraft, a nosedown auxiliary pitching moment and a roll-right auxiliary rolling moment produced reductions in the range of 15–65% in all components of vibratory hub loads. For both aircraft, the nosedown auxiliary pitching moment increased the nosedown pitch attitude of the aircraft and reduced the rotor longitudinal cyclic flapping and the longitudinal cyclic pitch input. For the BO-105, the roll-left auxiliary moment increased the leftward shaft tilt and no longer required the tip path plane to tilt left relative to the hub plane. This decreased the lateral cyclic pitch input. However, for the UH-60, the roll-right auxiliary moment actually reversed the roll attitude of the aircraft (shaft now tilting right). This required a large leftward tilt of the tip path plane relative to the hub plane and increased the lateral cyclic pitch requirement. When implementation of the auxiliary moments through collective and differential pitch inputs to the horizontal tail was examined, it was observed that the expected reductions in vibration were indeed achieved, but that the auxiliary roll moment generated was smaller than expected due to one-half of the horizontal tail being stalled.

Nomenclature

a	=	lift curve slope of main rotor blades
a_{ht}	=	lift curve slope of horizontal tail
D_F	=	fuselage drag parallel to flight direction, positive aft
D_{ht}	=	horizontal tail drag in flight direction, positive aft
F_x	=	main rotor drag, positive aft
F_y	=	main rotor side force, positive right
F_z	=	main rotor thrust, positive up
J	=	vibration index
L_F	=	fuselage lift perpendicular to the flight direction
M_x	=	main rotor rolling moment, positive roll left
M_x^A	=	auxiliary rolling moment, positive roll left
M_y	=	main rotor pitching moment, positive nose up
M_y^A	=	auxiliary pitching moment, positive nose up
M_{y_F}	=	fuselage pitching moment, positive nose up
M_z	=	main rotor yaw moment, positive nose yaw left
m_0	=	blade mass per unit length
N_b	=	number of blades on the main rotor
R	=	main rotor radius
S_F	=	fuselage flat plate area
S_{ht}	=	horizontal tail area
T_{ht}	=	horizontal tail download perpendicular to flight direction, positive down
T_{tr}	=	tail rotor thrust, positive to the right
V_x	=	air velocity at the horizontal tail in direction of flight, positive aft
V_z	=	air velocity at the horizontal tail perpendicular to direction of flight, positive down
W	=	vehicle weight
$\bar{w}_0, \beta_0$	=	rotor coning
$\bar{w}_{1c}, \beta_{1c}$	=	tip path plane longitudinal tilt (longitudinal cyclic flapping)
$\bar{w}_{1s}, \beta_{1s}$	=	tip path plane lateral tilt (lateral cyclic flapping)
$x_{\text{c.g.}}$	=	longitudinal offset of the c.g. ahead of the rotor hub
x_{ht}	=	longitudinal offset of the horizontal tail aft of the c.g.
x_{tr}	=	longitudinal offset of the tail rotor aft of the c.g.
$y_{\text{c.g.}}$	=	lateral offset of the c.g. to the right of the rotor hub
$z_{\text{c.g.}}$	=	vertical offset of the c.g. below the rotor hub
z_{ht}	=	vertical offset of the horizontal tail above the c.g.
z_{tr}	=	vertical offset of the tail rotor above the c.g.
α_{ht}	=	horizontal tail angle of attack, positive nose down
α_i	=	built-in incidence of horizontal tail relative to the waterline, positive nose down
α_s	=	longitudinal shaft tilt, positive nose down
α_{s_i}	=	Built-in shaft tilt relative to the waterline, positive nose-down

Received 23 January 2003; revision received 26 July 2003; accepted for publication 24 September 2003.

*Associate Professor, Rotorcraft Center of Excellence, Department of Aerospace Engineering, 229 Hammond Building; fgandhi@psu.edu. Senior Member AIAA.

†Research Engineer, U.S. Army Vehicle Technology Directorate.

α_{wl} = fuselage (waterline) longitudinal tilt, positive nose down
γ = Lock number
δ_c = horizontal tail collective pitch, positive nose down
δ_d = horizontal tail differential pitch, positive nose down on right side
θ_{tr} = tail rotor collective pitch
θ_{1c} = main rotor lateral cyclic pitch
θ_{1s} = main rotor longitudinal cyclic pitch
θ_{75} = main rotor collective pitch
λ = inflow ratio
ν_β = first rotating flap frequency
σ = main rotor solidity
ϕ_s = side shaft tilt, positive roll right
Ω = main rotor angular velocity

Superscripts

0 = steady component of rotor hub loads
$4P$ = four per revolution component of rotor hub loads

I. Introduction

IN moderate- to high-speed flight conditions, helicopters can experience severe vibration levels due to the rotor blades operating in a nonaxisymmetric aerodynamic environment. The periodic inertial and aerodynamic loading experienced by the rotor blades is transmitted, in part, to the rotor hub at harmonics of the blade passage frequency, $N_b\Omega$. (N_b is the number of blades and Ω is the rotor frequency.) The vibratory loads transmitted to the rotor hub can result in significant crew and passenger discomfort, increased component fatigue and maintenance requirements, and reduced effectiveness of sensitive equipment and weapon systems for military helicopters. Accordingly, considerable effort has been devoted over the past several decades to examine passive design and active control strategies for helicopter vibration reduction.[1–4] Passive methods have included the use of vibration absorbers and isolators, as well as structural and aerodynamic design optimization of rotor blades. Although these methods can be successful, they generally involve a weight penalty, and their performance can degrade with changes in operating conditions. Active methods, such as higher harmonic blade pitch control, or individual blade control (IBC) can be very effective and have the ability to adapt to changes in operating condition, but they often have large power requirements produce large pitch link loads, and involve considerable complexity (such as transmission of power to the rotating system through a slip ring, for IBC). Another active strategy, active control of structural response (ACSR), places actuators in the fixed system to cancel the incoming N_b per revolution hub loads. ACSR can reduce airframe vibrations locally, but may also have high-power and actuation requirements and leaves the dynamic stresses experienced by the rotor blades unaltered.

Another approach considered involves changing the configuration, for example, tilting the rotors forward into propeller mode as in the case of tilt-rotor aircraft, or introducing auxiliary lift, auxiliary thrust, or both, as in the case of compound helicopters. In tilt-rotor aircraft, tilting the rotors into propeller mode (and having the fixed wings provide all of the lift) puts them in a virtually axisymmetric aerodynamic environment, thereby eliminating the source of vibration. This also eliminates compressibility and stall problems that limited the maximum flight speed (the main reason for tilting the rotors to propeller mode). Of course, the complexity involved in tilting the rotors is immense, and, from that perspective, helicopter compounding represents a more incremental design evolution. Conventional helicopter compounding, achieved by introduction of auxiliary lift (through fixed wings), auxiliary thrust (through pusher or tractor propellers or jet engines), or a combination thereof, offloads the main rotor and has been reported to reduce vibration levels, particularly in the case of thrust compounding.[5–8] In a recent study, the changes in vehicle trim and the reductions in vibration achievable by the use of lift, thrust, and full compounding were compared, and the underlying physics for each case was discussed in detail.[9] Helicopter compounding, as a concept, has its own set of drawbacks. For example, compound lift configurations have a low-speed performance penalty due to wing–wake interference, and compound thrust configurations have greater complexity associated with the auxiliary propulsion. In both cases, there is a considerable weight penalty as well, and such issues can make compound helicopters prohibitive for short-range or moderate- to low-speed missions.[10]

Most of the observations in the literature on changes in vibration levels due to lift, thrust, or full compounding generally attributed the reductions to the unloading of the rotor (because it is no longer required to support the entire aircraft weight and/or provide the propulsive thrust of the aircraft). Sekula and Gandhi,[9] however, associated the reductions for the different types of compound configurations to the changes in vehicle attitude and control settings in each case. Whereas it is easy to appreciate that the rotor response and the hub vibrations will vary with the vehicle attitude and the main rotor pitch controls, these are not parameters that can be arbitrarily varied. They are determined based on vehicle equilibrium (trim) considerations. From this standpoint, introduction of auxiliary lift, thrust, or both, allow variation in vehicle attitude and rotor pitch controls, while still satisfying vehicle equilibrium. The results in Ref. 9 also indicated that maximum reductions in vibration, seen with thrust compounding, were accompanied by significant reductions in rotor cyclic pitch inputs.

The present study examines a new idea, namely, the introduction of auxiliary moments in the fixed system (through aerodynamic surfaces, for example), which enables changes in the vehicle attitude and rotor pitch controls to reduce rotor hub vibratory loads. It is recognized that the rotor cyclic pitch controls provide steady rotor hub pitching and rolling moments to tilt the thrust vector in the required direction for equilibrium. Thus, if auxiliary pitching and rolling moments in the fixed system could change the aircraft attitude and contribute to the tilting of the thrust vector, this would free up the rotor cyclic pitch controls and still satisfy vehicle equilibrium. In other words, rather than being encumbered with a set of rotor cyclic pitch inputs that satisfy equilibrium but that are suboptimal from a vibrations standpoint, rotor pitch inputs that minimize vibrations could be sought and fixed-system auxiliary moments used to help satisfy vehicle equilibrium. The reason auxiliary moments are being considered, rather than auxiliary lift or thrust (used in conventional compound helicopters), is the very low additional cost. It is anticipated that the required moments could be introduced by simply changing the pitch setting of the horizontal tail, or deflecting trailing-edge flaps on it. Pitching moments could be introduced by deployment of both halves of the horizontal tail collectively (like elevators), and rolling moments could be introduced by differential deployment (like ailerons). Because most flying helicopters already have horizontal tails, there is little additional weight, complexity, and performance penalty (due to the interference between the wake and a large fixed wing in compound lift configurations). In the event that the auxiliary moments generated by the horizontal tail are insufficient in magnitude, small alterations to existing aircraft could be made, such as an increase in the horizontal tail size, movement of its location, or augmentation of it with a small forward canard.

Although fixed-system control surfaces have been considered for augmentation of traditional helicopter flight controls in the past, a detailed examination of the impact of auxiliary moments on the vibratory hub loads is not available in the literature. The only results available were very limited in nature, but did demonstrate that changing the incidence of the trailing edge of the right-hand stabilizer influenced the vertical vibrations of the Lockheed Cheyenne.[7] The present study has three basic goals. First, comprehensively examine the effects of the introduction of auxiliary pitching moments, rolling moments, and a combination of both on all components of the main rotor vibratory hub loads, at moderate- to high-speed flight conditions. Second, for the levels of auxiliary moments that produced maximum vibration reductions, examine the changes in trim (individual control settings and vehicle attitude) that enabled these reductions. Third, develop a fundamental understanding of the underlying mechanisms involved that produced the changes in trim

and the reductions in vibration with auxiliary pitching and rolling moments. The analysis is carried out for two different types of helicopters, a lightweight BO-105-type hingeless rotor helicopter and a medium-weight UH-60-type articulated rotor helicopter. The results in this paper are meant to be general, to highlight the vibration reductions possible, and to provide an explanation of the physics of the problem. Thus, there is no emphasis on implementation details such as location and sizing of the horizontal tail or canard, or any weight and drag penalty that may be associated. Therefore, fixed-system auxiliary moments are considered in the mathematical model without specification of how exactly they would be achieved. Only in Sec. III.B.4 is implementation examined through the horizontal tail for the UH-60-type helicopter.

II. Analysis

To evaluate the effectiveness of auxiliary pitching and rolling moments in reducing helicopter hub vibration, a comprehensive rotorcraft aeroelastic analysis based on the UMARC formulation[11] is used. In the analysis, the rotor blades are assumed to undergo elastic flap and lag bending and elastic torsion deformation. The blades are discretized along the span by the use of the finite element method. Blade-element theory is used to calculate the sectional aerodynamic loads acting on the rotor blades, with a table lookup routine (which accounts for compressibility effects and static stall) used to obtain the circulatory lift, drag, and pitching moment. The model also takes into consideration the noncirculatory lift and pitching moment and the reverse flow region on the retreating side of the disk. The discretized blade equations of motion are transformed to modal space to reduce computational cost, and the blade periodic response in forward flight is calculated by the use of the temporal finite element method. After calculation of the periodic response, the blade loads can then be integrated along the span to obtain the blade root loads, and these can be integrated around the azimuth and summed over the N blades of the rotor to calculate the rotor hub loads (the hub forces F_x^0, F_y^0, and F_z^0 and moments M_x^0, M_y^0, and M_z^0). The rotor hub loads appear in the vehicle equilibrium (trim) equations and impact the vehicle orientation (pitch attitude α_{wl} and roll attitude or lateral shaft tilt ϕ_s) and control settings (collective pitch θ_{75}, longitudinal cyclic pitch θ_{1s}, lateral cyclic pitch θ_{1c}, and tail rotor collective pitch θ_{tr}). Evaluation of blade response and vehicle orientation and controls is carried out iteratively in a coupled response–trim calculation procedure because the blade response influences the steady rotor hub loads that impact the vehicle orientation and control settings, and the attitude and controls, in turn, affect the blade response. The iterative process continues until convergence, with the converged solution yielding the vehicle orientation and controls, blade periodic response, as well as the steady and vibratory hub loads. Figure 1 shows all of the forces and moments acting on the vehicle, and the vehicle equilibrium equations are then obtained by summation of the forces and moments at the rotor hub.

In the present study, the influence of auxiliary pitching and rolling moments on the rotor hub vibratory loads was examined for two different configurations: 1) a light (5800 lb) BO-105-type helicopter with a four-bladed hingeless rotor and 2) a larger (16800 lb) UH-60-type helicopter with a four-bladed articulated rotor. The rotor and fuselage properties for these two configurations are presented in Tables 1 and 2, respectively. The vehicle equilibrium equations for the UH-60 helicopter are given hereafter and have been properly modified to include the auxiliary moments:

$$\sum F_x = F_x^0 \cos\left(\alpha_{\mathrm{wl}} + \alpha_{s_i}\right) - F_z^0 \sin\left(\alpha_{\mathrm{wl}} + \alpha_{s_i}\right) + D_F + D_{\mathrm{ht}} = 0$$

$$\sum F_y = F_y^0 \cos\phi_s + F_z^0 \sin\phi_s + T_{\mathrm{tr}} \cos\phi_s + L_F \sin\phi_s - T_{\mathrm{ht}} \sin\phi_s = 0$$

$$\sum F_z = F_z^0 \cos\phi_s \cos\left(\alpha_{\mathrm{wl}} + \alpha_{s_i}\right) + F_x^0 \sin\left(\alpha_{\mathrm{wl}} + \alpha_{s_i}\right) - W + L_F \cos\phi_s - F_y^0 \sin\phi_s - T_{\mathrm{ht}} \cos\phi_s - T_{\mathrm{tr}} \sin\phi_s = 0$$

$$\sum M_x = M_x^0 \cos\alpha_{s_i} - M_z^0 \sin\alpha_{s_i} + T_{\mathrm{tr}}(z_{\mathrm{c.g.}} - z_{\mathrm{tr}}) + W(z_{\mathrm{c.g.}} \sin\phi_s - y_{\mathrm{c.g.}} \cos\phi_s) + \underline{M_x^A} = 0$$

$$\sum M_y = M_y^0 + M_{y_F} - D_F(z_{\mathrm{c.g.}} \cos\alpha_{\mathrm{wl}} + x_{\mathrm{c.g.}} \sin\alpha_{\mathrm{wl}}) - D_{\mathrm{ht}}[(z_{\mathrm{c.g.}} - z_{\mathrm{ht}}) \cos\alpha_{\mathrm{wl}} - (x_{\mathrm{ht}} - x_{\mathrm{c.g.}}) \sin\alpha_{\mathrm{wl}}] + T_{\mathrm{ht}}[(x_{\mathrm{ht}} - x_{\mathrm{c.g.}}) \cos\alpha_{\mathrm{wl}} + (z_{\mathrm{c.g.}} - z_{\mathrm{ht}}) \sin\alpha_{\mathrm{wl}}] + W(z_{\mathrm{c.g.}} \sin\alpha_{\mathrm{wl}} - x_{\mathrm{c.g.}} \cos\alpha_{\mathrm{wl}}) + \underline{M_y^A} = 0$$

$$\sum M_z = M_z^0 \cos\alpha_{s_i} + M_x^0 \sin\alpha_{s_i} + T_{\mathrm{tr}}(x_{\mathrm{tr}} - x_{\mathrm{c.g.}}) - (D_F \cos\alpha_{\mathrm{wl}} - W \sin\alpha_{\mathrm{wl}}) y_{\mathrm{c.g.}} - W \cos\alpha_{\mathrm{wl}} \sin\phi_s x_{\mathrm{c.g.}} = 0 \tag{1}$$

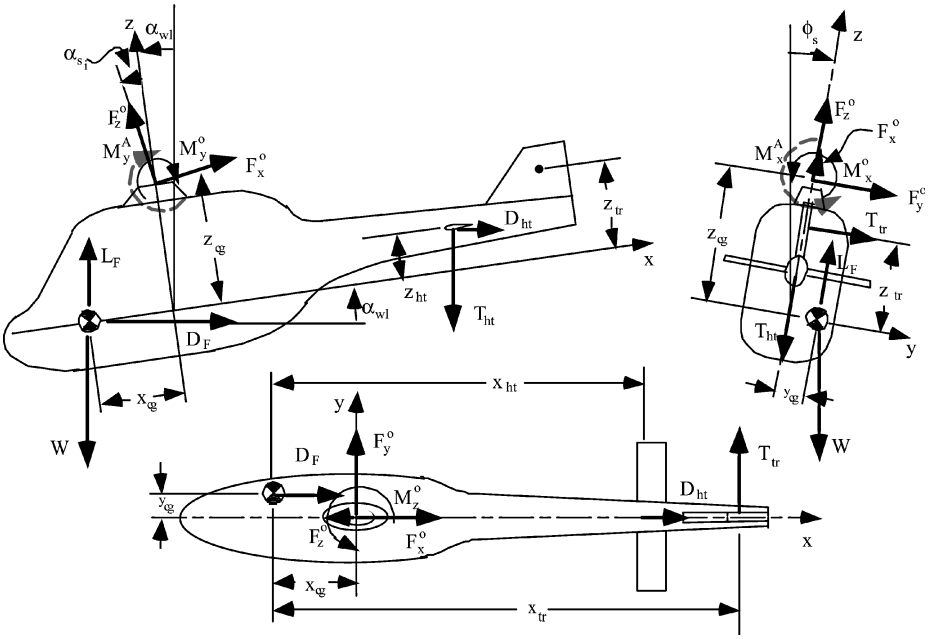

Fig. 1 Equilibrium forces and moments acting on the helicopter.

Table 1 Properties of the BO-105 type helicopter

Property	Value
Helicopter	
Weight W	5800 lb
Longitudinal c.g. offset $x_{\text{c.g.}}$	0 ft
Lateral c.g. offset $y_{\text{c.g.}}$	0 ft
Vertical c.g. offset $z_{\text{c.g.}}$	3.24 ft
Fuselage flat-plate area S_F	8.25 ft^2
Rotor	
Blade number N_b	4
Radius R	16.2 ft
Chord c	1.29 ft
Solidity σ	0.1
Blade mass m_0	0.27 slugs/ft
Linear twist θ_{tw}	0 deg
Angular velocity Ω	40.123 rad/s
Lock number γ	6.34
Reference lift coefficient a	5.73
Airfoil	NACA 0012
Nondimensional rotating frequencies	
First flap ν_β	1.11
First lag ν_ζ	0.61
First torsion ν_ϕ	3.29
Horizontal tail	
Area S_{ht}	9.07 ft^2
Reference lift coefficient a_{ht}	6.0
Incidence angle α_i	0 deg
Longitudinal offset x_{ht}	15.39 ft
Vertical offset z_{ht}	3.24 ft
Tail rotor	
Reference lift coefficient a_{tr}	6.0
Angular velocity Ω_{tr}	5Ω
Rotor radius R_{tr}	3.24 ft
Solidity σ_{tr}	0.15
Longitudinal offset x_{tr}	19.44 ft
Vertical offset z_{tr}	3.24 ft

Table 2 Properties of the UH-60 type helicopter

Property	Value
Helicopter	
Weight W	16,800 lb
Longitudinal c.g. offset $x_{\text{c.g.}}$	−1.525 ft
Lateral c.g. offset $y_{\text{c.g.}}$	0 ft
Vertical c.g. offset $z_{\text{c.g.}}$	5.825 ft
Rotor	
Blade number N_b	4
Radius R	26.8 ft
Chord c	1.73 ft
Solidity σ	0.082
Blade mass m_0	0.2357 slug/ft
Linear twist θ_{tw}	−18 deg
Angular velocity Ω	27.05 rad/s
Built-in shaft tilt α_{s_i}	3 deg
Lock number γ	8.0
Reference lift coefficient a	5.73
Airfoil	SC 1095
Nondimensional rotating frequencies	
First flap ν_β	1.04
First lag ν_ζ	0.271
First torsion ν_ϕ	4.27
Horizontal tail	
Area S_{ht}	45 ft^2
Reference lift coefficient a_{ht}	6.0
Incidence angle α_i	−5.45 deg
Longitudinal offset x_{ht}	28.4 ft
Vertical offset z_{ht}	−0.09 ft
Tail rotor	
Reference lift coefficient a_{tr}	6.0
Angular velocity Ω_{tr}	5Ω
Rotor radius R_{tr}	5.5 ft
Solidity σ_{tr}	0.188
Longitudinal offset x_{tr}	31.04 ft
Vertical offset z_{tr}	6.63 ft

Detailed expressions for the fuselage lift L_F, drag D_F, and pitching moment M_{y_F}, as well as the horizontal tail download T_{ht} and drag D_{ht}, are obtained from Ref. 12. Clearly, the auxiliary rolling moment M_x^A and pitching moment M_y^A, underlined for clarity, will have an effect on the vehicle trim (orientation and controls), which, in turn, will have an influence on the blade response and the rotor vibrations.

For the BO-105 helicopter, several additional simplifying assumptions have been made to achieve the clearest possible understanding of the physical mechanisms involved. First, α_{s_i}, the built-in main rotor shaft tilt (relative to the waterline), is assumed to be zero. Thus, as the aircraft pitches, the waterline angle and the main rotor shaft tilt are the same, and these are denoted by α_s. In addition to setting $\alpha_{s_i} = 0$ and $\alpha_{\text{wl}} = \alpha_s$ in Eq. (1), it is assumed that the fuselage lift and pitching moment are zero, the fuselage drag is independent of vehicle attitude ($D_F = \frac{1}{2}\rho V^2 S_F$, depending only on the airspeed and the equivalent fuselage flat plate area S_F), and the horizontal tail produces only a download ($T_{\text{ht}} = \frac{1}{2}\rho V^2 S_{\text{ht}} a_{\text{ht}} \alpha_s$) and no drag ($D_{\text{ht}}$ is assumed to be zero). The c.g. is assumed to be directly below the hub ($x_{\text{c.g.}} = 0$, $y_{\text{c.g.}} = 0$), and the tail rotor vertical offset below the main rotor hub, $z_{\text{c.g.}} - z_{\text{tr}}$, is zero, so that the tail rotor does not produce any rolling moment around the rotor hub. With these simplifications for the BO-105, the vehicle equilibrium equations (1) can be reduced to

$$\sum F_x = F_x^0 \cos\alpha_s - F_z^0 \sin\alpha_s + D_F = 0$$

$$\sum F_y = F_y^0 \cos\phi_s + F_z^0 \sin\phi_s + T_{\text{tr}} \cos\phi_s - T_{\text{ht}} \sin\phi_s = 0$$

$$\sum F_z = F_z^0 \cos\phi_s \cos\alpha_s + F_x^0 \sin\alpha_s - T_{\text{ht}} \cos\phi_s - W - F_y^0 \sin\phi_s - T_{\text{tr}} \sin\phi_s = 0$$

$$\sum M_x = M_x^0 + W z_{\text{c.g.}} \sin\phi_s + \underline{M_x^A} = 0$$

$$\sum M_y = M_y^0 - D_F z_{\text{c.g.}} \cos\alpha_s + W z_{\text{c.g.}} \sin\alpha_s + T_{\text{ht}}[x_{\text{ht}} \cos\alpha_s + (z_{\text{c.g.}} - z_{\text{ht}}) \sin\alpha_s] + \underline{M_y^A} = 0$$

$$\sum M_z = M_z^0 + T_{\text{tr}} x_{\text{tr}} = 0 \tag{2}$$

It is envisioned that the auxiliary moments in the fixed system would be introduced by a change of the incidence of the horizontal tail, or deflection of the control surfaces on the horizontal tail (functioning much like ailerons and elevators). Alternatively, a horizontal tail and a forward canard wing could be used in combination. In principle, some lift and drag could be introduced in addition to the moments, and if a canard is added or the horizontal tail enlarged, there could be weight, sizing, placement, and interference issues to consider. However, these effects are expected to be much smaller than would be the case for conventional lift or thrust compounding, and they are neglected in the present study. This is also in keeping with the emphasis, which is not on the implementation details but rather on the development of a very fundamental understanding of the mechanism causing the changes in trim and reduction in vibration when auxiliary moments are used. Thus, for all of the results in Sec. III.A (for the BO-105) and III.B.1–III.B.3 (for the UH-60) fixed-system auxiliary moments M_x^A and M_y^A are introduced without any specification of how they would be applied. The conclusions drawn are meant to be broad and general, rather than limited to a specific design. Only in Sec. III.B.4 is the implementation considered via the horizontal tail on the UH-60 aircraft.

To examine the effectiveness of fixed-system auxiliary moments in reducing helicopter hub vibratory loads, a composite vibration index J is defined as follows:

$$J = K\sqrt{\left(F_x^{4P}\right)^2 + \left(F_y^{4P}\right)^2 + \left(F_z^{4P}\right)^2 + \left(M_x^{4P}\right)^2 + \left(M_y^{4P}\right)^2 + \left(M_z^{4P}\right)^2} \tag{3}$$

In Eq. (3), the individual components of the four per revolution vibratory hub forces are nondimensionalized by the factor $m_0\Omega^2R^2$ and the four per revolution vibratory moments by $m_0\Omega^2R^3$. A scaling factor K was used to set the vibration index for the baseline case (no auxiliary moments) equal to 100. Therefore, a vibration index of less than 100 indicates an overall decrease in vibration, whereas values greater than 100 indicate an increase.

III. Results and Discussion

A. Study on a BO-105-Type Aircraft

For the BO-105-type helicopter (whose properties are given in Table 1), Fig. 2 shows the influence of the auxiliary pitching and rolling moments on the vibration index J at an advance ratio of 0.35 (135 kn). When an auxiliary pitching moment alone is considered ($M_x^A = 0$), it is seen that maximum reduction in vibration index J is obtained for a nose-down moment of $M_y^A = -7500$ ft · lb (case 1). On the other hand, if an auxiliary rolling moment alone is considered ($M_y^A = 0$), the maximum reduction in vibration index is obtained when a roll-left moment of $M_x^A = 6500$ ft · lb is applied (case 2). The largest decrease in vibration index (J reduced to a value of 37.0) is observed for a combination of an auxiliary rolling moment of $M_x^A = 7500$ ft · lb (roll-left), and an auxiliary pitching moment of $M_y^A = -7000$ ft · lb (nose-down pitch). This optimum combination of moments is hereafter referred to as case 3. A second region of overall vibration reduction is observed when a combination of a nose-up auxiliary pitching moment and a roll-right auxiliary rolling moment is used. In this case, the vibration index is reduced to $J = 57.3$ when $M_x^A = -28{,}500$ ft · lb and $M_y^A = 12{,}000$ ft · lb (case 4). Tables 3, 4, and 5, respectively, present the vibratory hub forces and moments, the helicopter attitude and control settings, and the tip flapping response for the baseline configuration (no auxiliary moments) and the four cases just outlined. The large magnitude of auxiliary moments required for case 4, as well as the excessive increase in the one per revolution flap response (Table 5) and rotor power (Table 4), make it an impractical candidate for vibration reduction, and this case will not be discussed further. A detailed analysis of cases 1–3 is provided in the following sections.

1. *Auxiliary Pitching Moment (Case 1)*

The optimum auxiliary pitching moment, $M_y^A = -7500$ ft · lb (nose-down), produced 20% reductions in the in-plane vibratory hub forces and a 33% reduction in the vibratory thrust but had a smaller impact on the vibratory hub moments (Table 3). The changes in the individual components of vibratory loads decreased the vibration index to a value of $J = 78.8$.

Note from Tables 4 and 5 that the auxiliary pitching moment has a significant impact on the longitudinal cyclic pitch θ_{1s}, the forward shaft tilt α_s, and the longitudinal cyclic flapping $\bar{w}_{1c}$. An examination of the pitching moment equilibrium of the vehicle (Table 6) provides a physical explanation of the changes that occurred. Note from Table 6 that the dominant pitching moments for the baseline configuration are a nose-down main rotor pitching moment M_y^0, balanced by the nose-up pitching moment from the horizontal tail download. When the relatively large nose-down auxiliary pitching moment, $M_y^A = -7500$ ft · lb is introduced, this increases the nose-down pitch attitude α_s of the aircraft. This, in turn, increases the longitudinal offset of the c.g. aft of the hub and the horizontal tail incidence and download, so that the nose-up pitching moment from

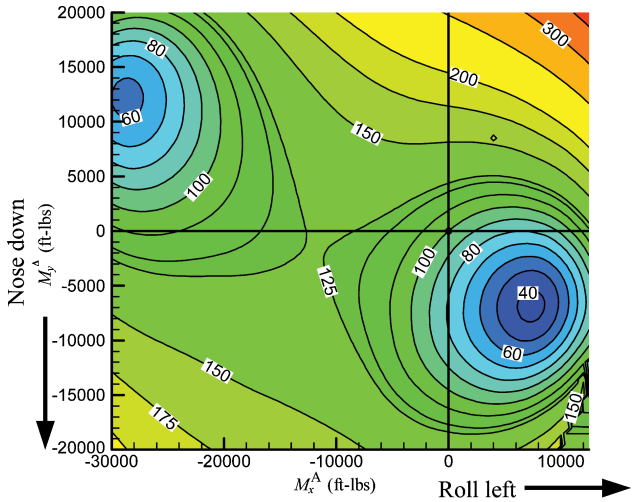

Fig. 2 Vibration index J vs auxiliary pitching and rolling moments at $\mu = 0.35$ for a BO-105-type helicopter.

Table 3 BO-105 vibratory hub loads

4/rev Vibratory hub force or moment	Baseline	Auxiliary pitch moment (case 1)	Auxiliary roll moment (case 2)	Case 3	Case 4
M_x^A, ft · lb	0	0	6,500	7,500	−28,500
M_y^A, ft · lb	0	−7,500	0	−7,000	12,000
J	*100*	*78.8*	*80.2*	*37.0*	*57.0*
F_x^{4P}					
lb	133	106	96	13	28
%	——	80	72	10	21
F_y^{4P}					
lb	146	113	107	10	37
%	——	78	73	7	25
F_z^{4P}					
lb	52	35	69	51	100
%	——	67	131	99	192
M_x^{4P}					
ft · lb	485	465	513	539	488
%	——	96	106	111	101
M_y^{4P}					
ft · lb	520	497	552	560	456
%	——	96	106	108	88
M_z^{4P}					
ft · lb	391	347	477	471	416
%	——	89	122	120	107

Table 4 BO-105 trim attitude and control settings and rotor power

Setting, deg	Baseline	Auxiliary pitch moment (case 1)	Auxiliary roll moment (case 2)	Case 3	Case 4
θ_{75}	8.92	8.82	9.36	9.39	8.38
θ_{1c}	3.30	2.76	1.72	0.99	11.88
θ_{1s}	−7.27	−5.66	−8.08	−6.79	−7.14
θ_{tr}	4.41	4.03	4.59	4.33	5.25
α_s	3.88	5.41	3.66	5.03	2.58
ϕ_s	−1.20	−1.23	−2.74	−3.01	6.53
λ	0.0340	0.0435	0.0326	0.0411	0.0257
Power, Hp	491	451	515	486	588

Table 5 BO-105 blade tip flapping response

Response, deg	Baseline	Auxiliary pitch moment (case 1)	Auxiliary roll moment (case 2)	Case 3	Case 4
$\bar{w}_0$	3.49	3.50	3.43	3.42	3.53
$\bar{w}_{1c}$	1.05	−0.73	0.98	−0.69	4.18
$\bar{w}_{1s}$	0.21	0.16	−1.69	−2.03	8.69
$\lvert\bar{w}_1\rvert$	1.07	0.75	1.95	2.14	9.64

Table 6 Components contributing to equilibrium of pitching moments for the BO-105 helicopter

Component, ft · lb	Baseline	Auxiliary pitch moment (case 1)	Auxiliary roll moment (case 2)	Case 3
M_y^0	−3154	2444	−2877	2423
$-D_F z_{\text{c.g.}} \cos(\alpha_s)$	−1666	−1662	−1666	−1663
$+W z_{\text{c.g.}} \sin(\alpha_s)$	1272	1772	1200	1647
$+T_{\text{ht}} x_{\text{ht}} \cos(\alpha_s)$	3547	4942	3344	4593
$+M_y^A$	0	−7500	0	−7000

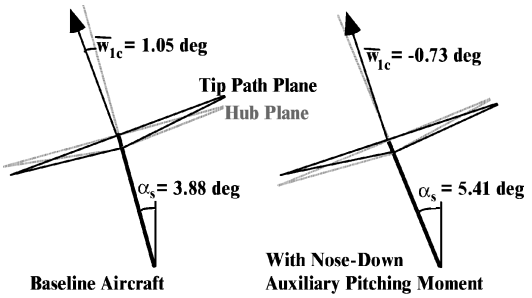

Fig. 3 Longitudinal tilt of the rotor shaft and the tip path plane for the baseline BO-105 and with auxiliary pitching moment.

the two sources is seen to increase (Table 6). Moreover, the direction of the main rotor pitching moment has now reversed (and is nose up) to satisfy equilibrium. The pitching moment from the fuselage drag remains unaffected due to the simplifying assumption that the fuselage drag (for this aircraft) was independent of the pitch attitude and varied only with forward speed.

Table 5 indicates that with the auxiliary pitching moment, the rotor longitudinal cyclic flapping $\bar{w}_{1c}$ actually changes sign, relative to the baseline. (Tip path plane now tilts backward relative to the rotor shaft.) For the baseline, the forward tilt of the main rotor thrust vector required to propel the aircraft forward was obtained from the moderate nose-down pitch attitude ($\alpha_s = 3.88$ deg) and the addition of positive longitudinal cyclic flapping ($\bar{w}_{1c} = 1.05$ deg) that resulted in the tip path plane tilting forward relative to the hub plane. With the auxiliary pitching moment, in contrast, a larger nose-down pitch attitude ($\alpha_s = 5.41$ deg) together with a negative longitudinal cyclic flapping ($\bar{w}_{1c} = -0.73$ deg, tip path plane tilting aft relative to the hub plane) produces the required forward tilt of the main rotor thrust (Fig. 3).

A simple analytical expression relating the rotor pitching moment coefficient to the longitudinal cyclic flapping response can be obtained for a rotor with uniform inflow and blades assumed to be undergoing rigid-body flapping rotations:

$$C_{M_y} = -(\sigma a/2\gamma)\left(\nu_\beta^2 - 1\right)\beta_{1c} \tag{4}$$

Although the comprehensive analysis in the present study assumes the blades undergo elastic deflections, Eq. (1) holds qualitatively, and the reversal in sign of the longitudinal cyclic flapping is then consistent with, and can be attributed to, the reversal in sign of the main rotor pitching moment M_y^0 (Table 6).

The longitudinal cyclic pitch θ_{1s}, of course, influences the longitudinal cyclic flapping $\bar{w}_{1c}$. For the baseline, the large negative longitudinal cyclic pitch ($\theta_{1s} = -7.27$ deg, Table 4) counters the natural tendency of the rotor to blow back in a wind and produces a net forward tilt of the tip path plane relative to the shaft. With the auxiliary pitching moment because the longitudinal cyclic flapping is smaller, it is reasonable to expect a significant reduction in the longitudinal cyclic pitch (θ_{1s} reduced to -5.66 deg; Table 4).

2. *Auxiliary Rolling Moment (Case 2)*

The optimum auxiliary rolling moment, $M_x^A = 6500$ ft · lb (roll left), produced reductions of nearly 30% in the in-plane vibratory hub forces and increases of about 20% in the vibratory yaw moment and 30% in the vertical vibratory hub force. It had little influence on the vibratory pitching and rolling moments (Table 3). The changes in the individual components of vibratory loads decreased the vibration index to a value of $J = 80.2$.

Note from Tables 4 and 5 that the auxiliary rolling moment has a significant impact on the lateral cyclic pitch θ_{1c}, the lateral shaft tilt ϕ_s, and the lateral cyclic flapping $\bar{w}_{1s}$. An examination the rolling moment equilibrium of the vehicle (Table 7) provides a physical explanation of the changes that occurred. Note from Table 7 that, for the baseline configuration, a roll-left moment from the main rotor, M_x^0, is balanced by a moment due to the lateral offset of the c.g., relative to the rotor hub, caused by the lateral tilt ϕ_s of the

Table 7 Components contributing to equilibrium of rolling moments for the BO-105 helicopter

Component, ft · lb	Baseline	Auxiliary pitch moment (case 1)	Auxiliary roll moment (case 2)	Case 3
M_x^0	395	404	−5596	−6514
$+W z_{\text{c.g.}} \sin(\phi_s)$	−393	−403	−899	−986
$+M_x^A$	0	0	6500	7500

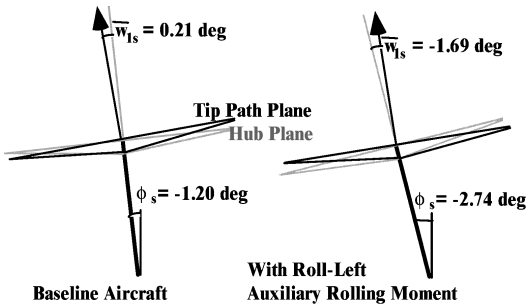

Fig. 4 Lateral tilt of the rotor shaft and the tip path plane for the baseline BO-105 and with auxiliary rolling moment.

rotor shaft. When the relatively large roll-left auxiliary moment, $M_x^A = 6500$ ft · lb, is introduced, this increases the lateral shaft tilt (or roll attitude) ϕ_s of the aircraft. Furthermore, it requires the main rotor rolling moment to undergo a reversal in sign (now a roll-right moment) and a significant increase in magnitude to satisfy equilibrium. The larger lateral shaft tilt also increases the rolling moment produced by the lateral offset of the c.g. relative to the rotor hub.

Analogous to Eq. (4), a simple analytical expression relating the rotor rolling moment coefficient to the lateral cyclic flapping response can be obtained:

$$C_{M_x} = (\sigma a/2\gamma)\left(\nu_\beta^2 - 1\right)\beta_{1s} \tag{5}$$

Clearly, the increase in magnitude and reversal in sign of the main rotor rolling moment M_x^0 with the introduction of the auxiliary rolling moment should be expected to produce a similar increase in magnitude and reversal in the sign of the lateral cyclic flapping. Table 5 indicates that this is indeed the case because $\bar{w}_{1s}$ changes from 0.21 to -1.69 deg.

For the baseline, the lateral tilt of the main rotor thrust vector required to counteract the tail rotor thrust was the result of a moderate roll-left attitude ($\phi_s = -1.20$ deg) and the addition of a small positive lateral cyclic flapping ($\bar{w}_{1s} = 0.21$ deg) that resulted in the tip path plane tilting left relative to the hub plane (Fig. 4). With the auxiliary rolling moment, in contrast, a larger roll left attitude ($\phi_s = -2.74$ deg) together with a negative lateral cyclic flapping ($\bar{w}_{1s} = -1.69$ deg, tip path plane tilting right relative to the hub plane) produces the required lateral tilt of the main rotor thrust.

With the change in the lateral cyclic flapping due to the auxiliary rolling moment, a reduction in the lateral cyclic pitch input θ_{1c} can be expected; this is observed in Table 4.

3. *Combination of Auxiliary Pitching and Rolling Moments (Case 3)*

When an optimum combination of auxiliary pitching and rolling moments, $M_y^A = -7000$ ft · lb (nose down) and $M_x^A = 7500$ ft · lb (roll-left), was introduced, reductions of over 90% in the in-plane vibratory hub forces were observed. The vibratory vertical hub force and pitching and rolling moments were relatively uninfluenced, whereas a 20% increase in the vibratory hub yawing moment was observed (Table 3). The changes in the individual components of vibratory loads decreased the vibration index to a value of $J = 37.0$.

Note from Tables 4 and 5 that the combination of auxiliary pitching and rolling moments (case 3) results in changes in all of the main rotor pitch controls, θ_{75}, θ_{1s}, and θ_{1c}; both the longitudinal and

lateral shaft tilt, α_s and ϕ_s; and the longitudinal and lateral cyclic flapping, $\bar{w}_{1c}$ and $\bar{w}_{1s}$, relative to the baseline. The pitching and rolling moment equilibrium equations of the vehicle are examined (Tables 6 and 7) to obtain a physical understanding of the changes that occurred.

As in case 1, introduction of the large nose-down auxiliary pitching moment causes the aircraft to assume a more nose-down pitch attitude. [That is, α_s increases to 5.03 deg, compared to 3.88 deg for the baseline (Table 4).] Furthermore, the direction of the main rotor pitching moment M_y^0 is reversed (and is now nose up), to satisfy equilibrium (Table 6). The reversal in the direction of the main rotor pitching moment causes the change in the sign of the longitudinal cyclic flapping $\bar{w}_{1c}$ [consistent with Eq. (4)], and the magnitude of longitudinal cyclic pitch input θ_{1s} decreases because the tip path plane is no longer inclined forward relative to the hub plane.

Introduction of the auxiliary rolling moment causes an increase in the aircraft roll-left attitude. [Lateral shaft tilt ϕ_s takes a value of -3.01 deg, compared to -1.20 deg for the baseline (Table 4), as in case 2.] This further requires that the main rotor rolling moment M_x^0, undergo a reversal in sign (now a roll-right moment) and a significant increase in magnitude to satisfy equilibrium (Table 7). This change in the main rotor rolling moment produces the increase in magnitude and reversal in sign of the main rotor lateral cyclic flapping $\bar{w}_{1s}$ consistent with Eq. (5). [Now $\bar{w}_{1s}$ takes a value of -2.03 deg, compared to 0.21 deg for the baseline (Table 5).] Because the primary function of the lateral cyclic pitch θ_{1c} in a conventional helicopter is to tilt the tip path plane left to counteract the tail rotor thrust, and this leftward tilt is no longer required in the presence of the auxiliary moments, the lateral cyclic pitch input is also reduced (Table 4).

Table 4 also shows the rotor power for the baseline aircraft and for the configurations with auxiliary moments introduced. Note that the rotor power for case 3 is very close to that for the baseline. However, if an auxiliary rolling moment alone is used (case 2), or for the optimal combination of auxiliary pitching and rolling moments in case 4, the rotor power can increase considerably (by up to 20%), even while the vibratory hub loads are reduced. Figures 5 and 6 show the blade sectional angle of attack around the rotor disk for the baseline aircraft and for the combination of auxiliary moments considered (case 3). The angles of attack for case 3 show small increases on the retreating side and small decreases on the advancing side. Even the very small reductions in angle of attack on the advancing side may have a benefit because the Mach numbers in this region are very close to the drag divergence Mach number and compressibility effects are very prominent. However, note that the angles of attack around the disk do not show gross changes, relative

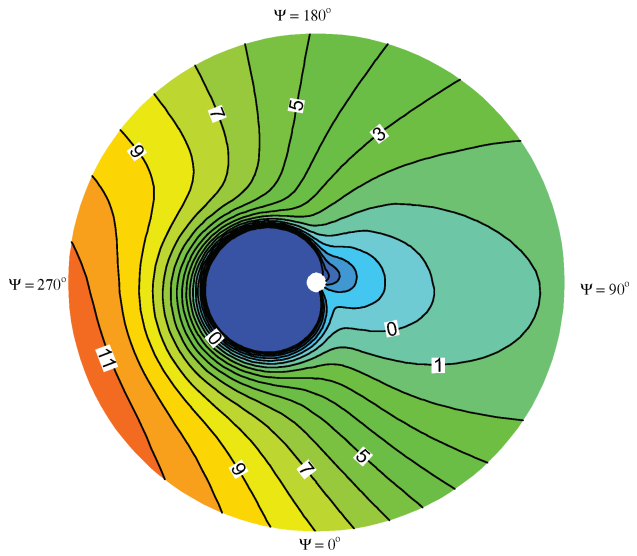

Fig. 5 Blade sectional angle of attack around the rotor disk for the baseline BO-105 rotor.

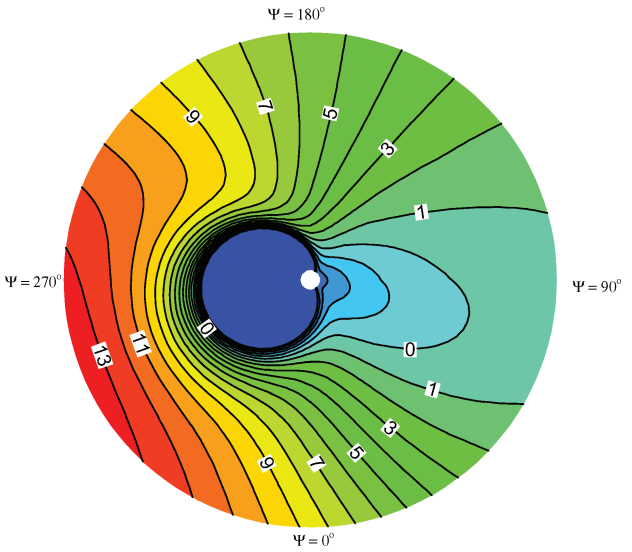

Fig. 6 Blade sectional angle of attack around the rotor disk for BO-105 rotor with auxiliary moments (case 3).

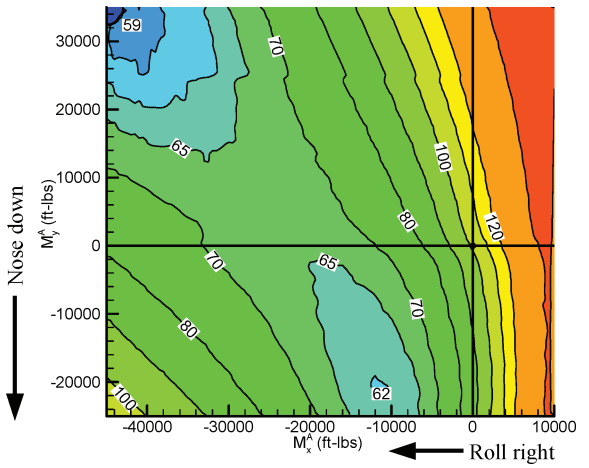

Fig. 7 Vibration index J vs auxiliary pitching and rolling moments at $\mu = 0.25$ for a UH-60-type helicopter.

to the baseline, as is the case when either auxiliary lift (lift compounding), auxiliary thrust (thrust compounding), or a combination thereof (full compounding) is used.[11]

B. Study on UH-60-Type Aircraft

For the UH-60-type helicopter (whose properties are given in Table 2), Fig. 7 shows the influence of the auxiliary pitching and rolling moments on the vibration index J at an advance ratio of 0.25 (107 kn). When an auxiliary pitching moment alone is considered ($M_x^A = 0$), it is seen that maximum reduction in vibration index J is obtained for a nose-down moment of $M_y^A = -21{,}000$ ft · lb (case 1). On the other hand, if an auxiliary rolling moment alone is considered ($M_y^A = 0$), the maximum reduction in vibration index is obtained when a roll-right moment of $M_x^A = -19{,}000$ ft · lb is applied (case 2). When auxiliary pitching and rolling moments are used in combination, there are two regions where significant reductions in vibration index are obtained as shown in Fig. 7. With a nose-down auxiliary pitching moment, $M_y^A = -20{,}500$ ft · lb, and a roll-right auxiliary moment, $M_x^A = -12{,}000$ ft · lb, the vibration index is reduced to a value of $J = 61.8$ (case 3). The largest decrease in vibration index (J reduced to 58.8) is observed for a combination of a nose-up pitching moment, $M_y^A = 32{,}000$ ft · lb, and a roll-right moment of $M_x^A = -43{,}000$ ft · lb (case 4). Tables 8, 9, and 10, respectively, list the vibratory hub forces and moments, the helicopter attitude and control settings, and the tip flapping response, for the

Table 8 UH-60 vibratory hub loads (lbs and ft · lbs)

4/rev Vibratory hub force or moment	Baseline	Auxiliary pitch moment (case 1)	Auxiliary roll moment (case 2)	Case 3	Case 4	Auxiliary moments through horizontal tail
M_x^A, ft · lb	0	0	−19,000	−12,000	−43,000	$\delta_d = 7.5$ deg
M_y^A, ft · lb	0	−21,000	0	−20,500	32,000	$\delta_c = -9.5$ deg
J	*100*	*86.1*	*66.1*	*61.8*	*58.9*	*68.7*
F_x^{4P}						
lb	329	297	145	236	207	93.8
%		90.2	44	71.7	62.9	28.4
F_y^{4P}						
lb	309	364	105	271	301	114
%		118	33.9	86.6	97.5	36.8
F_z^{4P}						
lb	623	178	625	300	252	505
%		28.7	100	48.2	40.5	81
M_x^{4P}						
ft · lb	1,345	547	1,562	887	1,193	1,383
%		40.7	116	65.9	88.7	103
M_y^{4P}						
ft · lb	1,548	623	1,879	1,029	1,548	1,675
%		40.2	121	66.4	80.5	108
M_z^{4P}						
ft · lb	144	86	89	52	60	49.7
%		59.9	61.8	36	86.3	34.5

Table 9 UH-60 trim attitude and control settings and rotor power

Settings, deg	Baseline	Auxiliary pitch moment (case 1)	Auxiliary roll moment (case 2)	Case 3	Case 4	Auxiliary moments through horizontal tail
θ_{75}	9.52	9.25	8.78	8.67	9.14	9.24
θ_{1c}	0.64	0.16	6.49	3.95	14.92	0.93
θ_{1s}	−6.45	−2.62	−5.99	−2.48	−10.71	−1.81
θ_{tr}	3.02	2.73	2.98	2.62	5.14	2.77
α_{wl}	−0.74	1.38	−1.02	1.03	−4.44	2.72
ϕ_s	−1.89	−1.74	1.16	0.29	3.49	−1.36
λ	0.0222	0.0313	0.021	0.0298	0.0059	0.0367
Power	1341	1219	1305	1161	2263	1234

Table 10 UH-60 blade tip flapping response

Response, deg	Baseline	Auxiliary pitch moment (case 1)	Auxiliary roll moment (case 2)	Case 3	Case 4	Auxiliary moments through horizontal tail
$\bar{w}_0$	3.43	3.32	3.44	3.34	3.54	3.17
$\bar{w}_{1c}$	3.88	0.68	3.31	0.41	7.4	0.01
$\bar{w}_{1s}$	−0.82	−0.94	4.55	2.4	12.3	−0.16
$\lvert\bar{w}_1\rvert$	3.97	1.16	5.63	2.43	14.4	0.16

baseline configuration (no auxiliary moments) and the four cases just outlined. The large magnitude of auxiliary moments required for case 4, as well as the excessive increase in the one per revolution flap response (Table 10) and rotor power (Table 9), make it an impractical candidate for vibration reduction, and this case will not be further discussed. A detailed analysis of cases 1–3 is provided in the following sections.

1. Auxiliary Pitching Moment (Case 1)

The optimum auxiliary pitching moment, $M_y^A = -21{,}000$ ft · lb (nose down), produced a 70% reduction in the vibratory thrust, 60% reductions in the vibratory hub pitching and rolling moments, and a 40% reduction in the vibratory hub yawing moment (Table 8). Its influence on the in-plane forces was smaller, and these changed by 10–20% relative to the baseline. The changes in the individual components of vibratory loads decreased the vibration index to a value of $J = 86.1$.

Introduction of the nose-down auxiliary pitching moment puts the aircraft in a nose-down pitch attitude (positive α_{wl}), as listed in Table 9. In contrast, the baseline UH-60 aircraft had a small nose-up pitch attitude at this flight speed, with the built-in forward tilt of rotor shaft and the longitudinal cyclic flapping providing the propulsive component of the thrust. Examining the pitching moment equilibrium of the vehicle (Table 11) provides a detailed physical explanation of the changes that occurred. For the baseline configuration, the main rotor produced a large nose-down pitching moment, which, in combination with the nose-down moments from the horizontal tail, fuselage drag, etc., countered the large nose-up moment due to the longitudinal offset of the c.g. aft of the rotor hub. With the nose-down auxiliary pitching moment, the main rotor pitching moment M_y^0 is drastically reduced. Furthermore, the new nose-down aircraft attitude produces a horizontal tail download and a nose-up pitching moment (in contrast to the baseline); this, together with an increased nose-up moment due to the aft c.g. offset, more or less balances the nose-down auxiliary moment, fuselage pitching moment, and moment due to the fuselage drag. Table 10 shows that the longitudinal cyclic flapping $\bar{w}_{1c}$ is drastically reduced relative to the baseline, and this is consistent with the reduction in the rotor pitching moment M_y^0, as suggested by Eq. (4). The reduction in longitudinal cyclic flapping, in turn, implies a reduction

Table 11 Components contributing to equilibrium of pitching moments for the UH-60 helicopter

Pitching moment about the rotor hub, positive nose up, ft · lb	Baseline	Auxiliary pitch moment (case 1)	Auxiliary roll moment (case 2)	Case 3	Auxiliary moments through horizontal tail
Main rotor M_y^0	−8,571	−456	−7,105	282	1,333
Fuselage M_{y_F}	−5,393	−3,295	−5,700	−3,583	−2,153
Fuselage drag[a]	−5,630	−5,623	−5,607	−5,590	−5,677
Helicopter weight[b]	24,357	27,962	23,868	27,372	30,228
Horizontal tail download[c]	−4,582	2,502	−5,329	1,577	−22,194
Horizontal tail drag[d]	−181	−68	−192	−76	−1,518
Auxiliary moment M_y^A	0	−21,000	0	−20,500	0

[a] $D_F[z_{\text{c.g.}}\cos(\alpha_{\text{wl}}) + x_{\text{c.g.}}\sin(\alpha_{\text{wl}})]$.
[b] $W[z_{\text{c.g.}}\sin(\alpha_{\text{wl}}) - x_{\text{c.g.}}\cos(\alpha_{\text{wl}})]$.
[c] $T_{\text{ht}}[(x_{\text{ht}} - x_{\text{c.g.}})\cos(\alpha_{\text{wl}}) + (z_{\text{c.g.}} - z_{\text{ht}})\sin(\alpha_{\text{wl}})]$.
[d] $D_{\text{ht}}[(z_{\text{c.g.}} - z_{\text{ht}})\cos(\alpha_{\text{wl}}) - (x_{\text{ht}} - x_{\text{c.g.}})\sin(\alpha_{\text{wl}})]$.

Table 12 Components contributing to equilibrium of rolling moments for the UH-60 helicopter

Rolling moment about the rotor hub, positive nose up, ft · lb	Baseline	Auxiliary pitch moment (case 1)	Auxiliary roll moment (case 2)	Case 3	Auxiliary moments through horizontal tail
Main rotor[a]	3,904	3,626	17,603	12,095	5,618
Tail rotor[b]	−658	−582	−654	−571	−602
Helicopter weight[c]	−3,235	−2,966	1,987	502	−2,326
Auxiliary moment M_x^A	0	0	−19,000	−12,000	−2,688[d]

[a] $M_x^0\cos(\alpha_{s_i}) - M_z^0\sin(\alpha_{s_i})$.
[b] $T_{\text{tr}}(z_{\text{c.g.}} - z_{\text{tr}})$.
[c] $W[z_{\text{c.g.}}\sin(\phi_s) - y_{\text{c.g.}}\cos(\phi_s)]$.
[d] Auxiliary roll moment from differential pitch of horizontal tail δ_d.

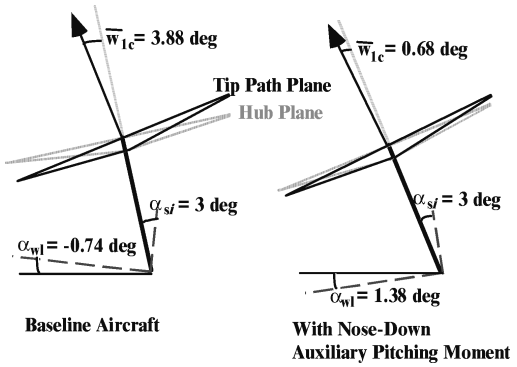

Fig. 8 Longitudinal tilt of the rotor shaft and the tip path plane for the baseline UH-60 and with auxiliary pitching moment.

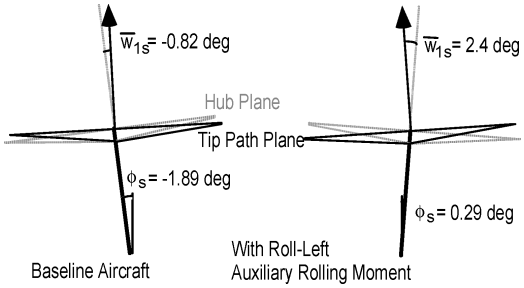

Fig. 9 Lateral tilt of the rotor shaft and the tip path plane for the baseline UH-60 and with auxiliary rolling moment.

in the longitudinal cyclic pitch input (from θ_{1s} of −6.45 deg for the baseline, to −2.62 deg, Table 9). Figure 8 shows how the combination of the aircraft pitch attitude and the longitudinal cyclic flapping produce the rotor propulsive force, for both the baselin and case 1.

Note that the BO-105, as well as the UH-60-type helicopters required nose-down auxiliary pitching moments for vibration reduction that put both aircraft in more of a nose-down pitch attitude. However, in the case of the BO-105, this reversed the main rotor pitching moment (to nose up) and resulted in an aft tilt of the tip path plane relative to the shaft. On the other hand, the nose-down main rotor pitching moment for the UH-60 was drastically reduced, but not reversed. This resulted in significantly reduced longitudinal cyclic flapping (very small forward tilt of the tip path plane relative to the shaft).

2. Auxiliary Rolling Moment (Case 2)

The optimum auxiliary rolling moment, $M_x^A = -19{,}000$ ft · lb (roll-right) produced 55–65% reductions in the in-plane vibratory hub forces and a 40% reduction in the vibratory hub yawing moment (Table 8). The vibratory thrust was virtually unchanged, and the vibratory hub pitching and rolling moments showed a 15–20% increase relative to the baseline. The changes in the individual components of vibratory loads decreased the vibration index to a value of $J = 66.1$.

As in the case of the BO-105, the auxiliary rolling moment significantly influences the lateral cyclic pitch θ_{1c}, the lateral shaft tilt ϕ_s, and the lateral cyclic flapping $\bar{w}_{1s}$, relative to the baseline (Tables 9 and 10). By examination of the rolling moment equilibrium of the vehicle (Table 12), it is seen that for the baseline configuration a roll-left moment from the main rotor is mostly balanced by a roll-right moment due to the lateral offset of the c.g. relative to the rotor hub, which together produce a leftward lateral shaft tilt negative [ϕ_s (Table 9)]. When the large roll-right auxiliary moment, $M_x^A = -19{,}000$ ft · lb is introduced, this reverses the lateral shaft tilt or roll attitude of the aircraft. [Now ϕ_s is positive (Table 9), that so the shaft now tilts rightward.] Furthermore, the main rotor rolling moment increases substantially in magnitude to satisfy equilibrium (Table 12). The larger main rotor rolling moment produces a substantially increased lateral cyclic flapping response (see Table 10), which, in turn, implies an increase in the lateral cyclic pitch input. In other words, θ_{1c} assumes a value of 6.49 deg, compared to 0.64 deg for the baseline (Table 9). Figure 9 shows how the combination of the aircraft roll attitude and the lateral cyclic flapping produce the rotor side force, for both the baseline and case 2.

Note that auxiliary rolling moments required for the BO-105- and the UH-60 type helicopters were distinctly different. In the case of the BO-105, the roll-left auxiliary moment increased the

leftward lateral shaft tilt and produced both a large roll-right main rotor rolling moment for equilibrium and a rightward tilt of the tip path plane relative to the hub plane. In contrast, the roll-right auxiliary moment for the UH-60 resulted in a rightward tilt of the rotor shaft and produced a large roll-left main rotor rolling moment for equilibrium, which, in turn, caused the tip path plane to tilt leftward relative to the rotor shaft.

3. Combination of Auxiliary Pitching and Rolling Moments (Case 3)

When an optimum combination of a nose-down auxiliary pitching moment, $M_y^A = -20{,}500$ ft · lb, and a roll-right auxiliary rolling moment, $M_x^A = -12{,}000$ ft · lb was introduced, reductions of the order of 15–30% in the in-plane vibratory hub forces, 50% in the vibratory vertical hub force, 35% in the vibratory hub pitching and rolling moments, and 65% in the vibratory hub yawing moment were observed (Table 8). The changes in the individual components of vibratory loads decreased the vibration index to a value of $J = 61.8$.

The data listed in Tables 9 and 10 indicate that this combination of auxiliary pitching and rolling moments produced changes in all of the main rotor pitch controls θ_{75}, θ_{1s}, and θ_{1c}; both the longitudinal and lateral shaft tilt α_s and ϕ_s; and the longitudinal and lateral cyclic flapping, $\bar{w}_{1c}$ and $\bar{w}_{1s}$, relative to the baseline. Examination of the pitching and rolling moment equilibrium equations of the vehicle (Tables 11 and 12) provides a clear understanding of the changes that occurred.

As in case 1, introduction of the nose-down auxiliary pitching moment causes the aircraft to assume a nose-down pitch attitude, where α_{wl} goes to 1.03 deg, compared to −0.74 deg for the baseline (Table 9). Furthermore, it is observed from Table 11 that the main rotor pitching moment M_y^0 is virtually eliminated; with the nose-up moments from the aft c.g. location and the horizontal tail download balancing out the nose-down fuselage pitching moment, moment due to the fuselage drag, and the auxiliary moment to satisfy equilibrium. As in case 1, the large reduction in the main rotor pitching moment M_y^0 significantly decreases the longitudinal cyclic flapping $\bar{w}_{1c}$ (Table 10); this, in turn, reduces the longitudinal cyclic pitch input requirement. That is, θ_{1s} changes from −6.45 deg for the baseline to −2.48 deg (see Table 9) because a large forward tilt of the tip path plane is no longer required, relative to the hub plane.

Introduction of the roll-right auxiliary rolling moment changes the direction of the lateral shaft tilt (rightward) and produces a roll-right aircraft attitude, that is, ϕ_s takes a value of 0.29 deg, compared to −1.89 deg for the baseline (Table 9). As in case 2, the main rotor rolling moment M_x^0 increases substantially in magnitude to satisfy equilibrium (Table 12). This produces a substantially increased lateral cyclic flapping response, where $\bar{w}_{1s}$ increases to 2.4 deg, compared to −0.82 deg for the baseline (Table 10), which, in turn, implies an increase in the lateral cyclic pitch input. For example, θ_{1c} assumes a value of 3.95 deg, compared to 0.64 deg for the baseline (Table 9). Although the changes in rolling moment equilibrium are qualitatively the same as those seen in case 2, they are all seen to a lesser degree because the auxiliary rolling moment used in case 3 was smaller. ($M_x^A = -12{,}000$ ft · lb, as compared to −19,000 ft · lb for case 2.) Thus, the main rotor roll-left moment, though larger than the baseline, is smaller than in case 2 (Table 12), and the lateral cyclic flapping and lateral cyclic pitch input are also similarly smaller than in case 2 (Tables 9 and 10).

The combination of auxiliary pitching and rolling moments in case 3 resulted in a 13.4% reduction in rotor power (Table 9). Smaller reductions were observed when individual auxiliary pitching and rolling moments were used. However, a prohibitive increase in rotor power was calculated for the large auxiliary moments of case 4. As was the case with the BO-105-type helicopter, the auxiliary pitching and rolling moments did not show any significant change in the blade sectional angles of attack around the rotor disk, relative to the baseline aircraft. (These results are not included.)

4. Auxiliary Moments Through the Horizontal Tail

In this section, auxiliary pitching and rolling moments are introduced through variations in the incidence angles of the left and the right halves of the horizontal tail. The UH-60 horizontal tail model was modified so that the incidence angle of each half of the tail could assume distinct values. However, rather than direct use of the incidence angles of the right and left halves, $\alpha_{\text{ht}}^{\text{right}}$ and $\alpha_{\text{ht}}^{\text{left}}$, respectively, as the independent variables, a collective pitch angle δ_c and a differential pitch angle δ_d were used as the independent variables. The net incidence angle of each half of the horizontal tail can then be written as

$$\alpha_{\text{ht}}^{\text{right}} = \alpha_{\text{wl}} + \alpha_i + \tan^{-1}(V_z/V_x)_{\text{ht}} + \delta_c + \delta_d \tag{6a}$$

$$\alpha_{\text{ht}}^{\text{left}} = \alpha_{\text{wl}} + \alpha_i + \tan^{-1}(V_z/V_x)_{\text{ht}} + \delta_c - \delta_d \tag{6b}$$

In Eq. (6), α_i is the baseline (built-in) incidence of the horizontal tail with respect to the fuselage waterline. (For the UH-60, $\alpha_i = -5.45$ deg, nose up.) The arctangent term accounts for change in the angle of attack due to wind, with empirical relations for V_z and V_x used from Ref. 12. The incidence angles were assumed to be uniform along the span of each half of the horizontal tail, and a table lookup procedure (which accounts for stall and poststall behavior) was used to calculate the aerodynamic coefficients for the NACA 0014 airfoil. Figure 10 defines all of the angles and wind velocities, for the right-half of the horizontal tail. Clearly, from Eqs. (6) and Fig. 10, a positive δ_c produces a download on (both halves of) the horizontal tail, which produces a nose-up (positive) pitching moment. A positive δ_d, on the other hand, increases the incidence angle and download on the right-half of the horizontal tail and decreases it on the left-half, resulting in a roll-right moment (negative rolling moment) on the aircraft. Thus, in the present section, a horizontal tail collective pitch δ_c and differential pitch δ_d are used to introduce the auxiliary pitching and rolling moments on the aircraft.

Figure 11 shows the influence of the horizontal tail collective and differential pitch angles on the vibration index J (at the advance ratio of 0.25, as in the preceding sections). The maximum reduction in vibration index ($J = 68.7$) is observed for a combination of $\delta_c = -9.5$ deg and $\delta_d = 7.5$ deg, with individual reductions of over 60–70% in the in-plane vibratory hub forces, 20% in the vibratory vertical hub force, and 65% in the vibratory hub yawing moment (Table 8). The vibratory hub pitching and rolling moments were relatively unaffected.

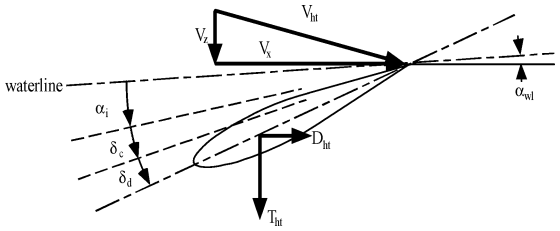

Fig. 10 Contributions to the aerodynamic incidence angle of the right half of horizontal tail of the UH-60-type aircraft.

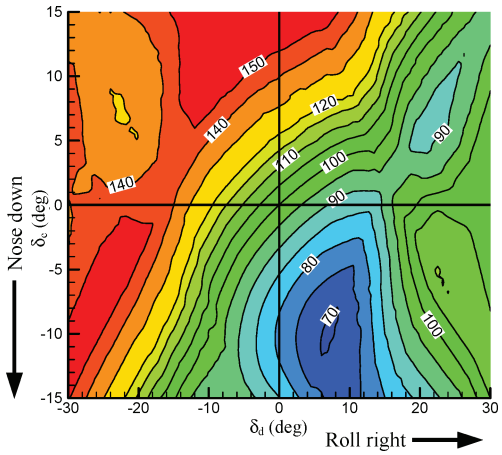

Fig. 11 Vibration index J vs horizontal tail collective and differential pitch settings for a UH-60-type helicopter.

Note that the horizontal tail collective pitch produced a nose-down (negative) auxiliary pitching moment, and the differential pitch produced a roll-right (negative) auxiliary rolling moment. Thus, the change in the trim of the helicopter was qualitatively similar to that of case 3. An examination of the pitching moment equilibrium (Table 11) shows that the nose-down pitching moment from the horizontal tail is about 17,500 ft · lb larger than that for the baseline UH-60 aircraft, and the total pitching moment it generates (around −22,000 ft · lb) is comparable to the nose-down auxiliary moments of cases 1 and 3. As in those cases, the aircraft assumes a more nose-down attitude ($\alpha_{\text{wl}} = 2.72$ deg, compared to −0.74 deg for the baseline; Table 9), which, in turn, significantly reduces the forward tilt of the tip path plane relative to the hub plane. (See the reduced longitudinal cyclic flapping $\bar{w}_{1c}$ in Table 10.) This requires a reduced longitudinal cyclic pitch input ($\theta_{1s} = -1.81$ deg, compared to −6.45 deg for the baseline; Table 9). Note in Table 11 that, as in cases 1 and 3, the main rotor pitching moment is significantly reduced compared to the baseline. Note that a negative δ_c is meant to reduce (or even make negative) α_{ht} in Eqs. (6). This produces an incremental horizontal tail upload and, therefore, a nose-down pitching moment on the aircraft. However, as the nose-down moment and pitch attitude of the aircraft start to increase (producing more positive α_{wl}), it is seen from Fig. 10 and Eqs. (6) that the effect of δ_c in decreasing α_{ht} is, in small part, negated. Also note that, unlike negative δ_c in preceding sections where auxiliary pitching moments were introduced independent of any auxiliary lift, here, the use of negative δ_c to generate a nose-down pitching moment produces a horizontal tail upload or an auxiliary lift in combination that offloads the main rotor somewhat. In the present case, the horizontal tail produces almost 600 lb more lift than does the baseline (Table 13). This results in a decrease in main rotor thrust from 16,653 lb (for the baseline) to 15,852 lb, a 5% reduction.

The horizontal tail differential pitch δ_d generates a 2688 ft · lb roll right auxiliary moment (Table 12). This rolling moment is considerably smaller than that seen in cases 2 and 3. Thus, it does not reverse the lateral shaft tilt from a roll-left to a roll-right attitude. [In this case, ϕ_s changed from −1.89 deg for the baseline UH-60 to positive values for cases 2 and 3 (Table 9).] However, it does reduce the aircraft roll-left attitude ($\phi_s = -1.36$ deg). Correspondingly, the increase in main rotor rolling moment, relative to the baseline, is smaller compared to that in cases 2 and 3 (Table 12). This also produces smaller changes in the lateral cyclic flapping (Table 10) and lateral cyclic pitch input (Table 9).

Table 13 Components contributing to equilibrium of vertical forces for the UH-60 helicopter

Component, ft	Baseline	Auxiliary moments through horizontal tail
$F_z^0 \cos(\phi_s) \cos(\alpha_s)$	16,625	15,760
$+F_x^0 \sin(\alpha_s)$	−13	39
$-W$	−16,800	−16,800
$+L_F \cos(\phi_s)$	5	238
$-T_{\text{ht}} \cos(\phi_s)$	154	736
$-F_y^0 \sin(\phi_s)$	−8	−8
$-T_{\text{tr}} \sin(\phi_s)$	27	28

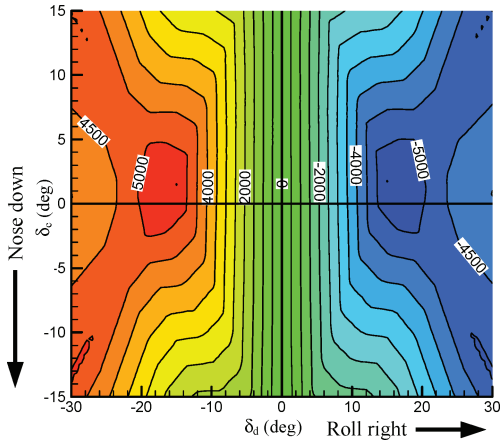

Fig. 12 Horizontal tail rolling moment (foot pounds) vs horizontal tail collective and differential pitch settings for UH-60-type helicopter.

Because the rolling moment generated with the horizontal tail is substantially lower than the auxiliary rolling moment, $M_x^A = -12{,}000$ ft · lb, in case 3 (comparable pitching moments) this issue is examined further. Figure 12 presents the horizontal tail rolling moment at varying values of δ_c and δ_d. An increase in the value of the differential pitch angle δ_d eventually causes the angle of attack on the right-half of the horizontal tail to reach the stall angle of the airfoil (approximately 15 deg). As the stall angle is reached, the ability of the horizontal tail to generate a larger rolling moment is reduced, and, in poststall, the rolling moment can actually decrease. If larger rolling moments are desired, the span of the horizontal tail would have to be increased, or a small wing (such as a canard) can be added that would not produce a large download in hover, yet could be used to generate a rolling moment.

IV. Summary

The present study examined the reductions in rotor hub vibratory loads that could be obtained through the introduction of auxiliary pitching and rolling moments in the fixed system. In a conventional helicopter, the aircraft attitude and pitch control inputs are required to satisfy vehicle force and moment equilibrium (trim) and may be less than optimal from a vibrations standpoint. The introduction of auxiliary moments allows change in vehicle attitude and control inputs, such that vibrations can be minimized, and vehicle equilibrium is still satisfied. Because auxiliary moments could be introduced by varying the pitch of, or controlling the trailing-edge flaps on, the right- and left-halves of the horizontal tail, the weight penalty, complexity, and performance losses associated with introduction of auxiliary lift and thrust (conventional compounding) would be alleviated. Vibration reductions by the use of auxiliary moments were examined on two different aircraft: 1) a light BO-105-type helicopter with a four-bladed hingeless rotor and 2) a medium-weight UH-60-type helicopter with a four-bladed articulated rotor. Vibration reductions were examined at a higher flight speed of 135 kn (corresponding to an advance ratio of 0.35) for the first aircraft, and at a moderate flight speed of 107 kn (corresponding to an advance ratio of 0.25) for the second aircraft. The observations from the numerical simulations in the present study are summarized hereafter.

For both the BO-105-type aircraft and the UH-60-type aircraft, auxiliary pitching and rolling moments of reasonable magnitude were able to reduce the rotor hub vibratory loads significantly, without producing excessive increase in blade flapping or cyclic pitch. For the BO-105, a nose-down auxiliary pitching moment, and a roll-left auxiliary rolling moment, individually, produced 20–30% reductions in the in-plane vibratory forces. When used in combination, reductions of around 90% in the in-plane vibratory forces were observed. The ability of the auxiliary moments to affect the hub vibratory pitching and rolling moments appeared to be very limited. For the UH-60, the auxiliary moments had a much wider influence on the vibratory hub loads. A nose-down auxiliary pitching moment reduced the four per revolution vertical hub force by 70% and the four per revolution hub pitching and rolling moments by 60%. A roll-right auxiliary rolling moment reduced the four per revolution hub in-plane forces by 55–60%. When the auxiliary moments were used in combination, simultaneous 15–30% reductions in in-plane hub forces, a 50% reduction in vertical hub force, and 35% reductions in hub pitching and rolling moments were observed. In addition, for the UH-60, reductions in vibratory yawing moments from 40 (when auxiliary pitching or rolling moments were used individually) to 65% (when they were used in combination) were obtained.

For both aircraft, the nose-down auxiliary pitching moment increased the nose-down pitch attitude or forward shaft tilt. This reduced the longitudinal cyclic flapping relative to the baseline. For the UH-60, the forward tilt of the tip path plane, relative to the hub plane, was reduced; but for the BO-105, the tip path plane actually had a slight backward tilt relative to the hub plane. For both aircraft,

significant reductions in the longitudinal cyclic pitch input θ_{1s} were observed.

The auxiliary roll moments required for the two aircraft were different. For the BO-105, a roll-left moment increased the leftward shaft tilt. Consequently, the tip path plane was no longer required to tilt leftward relative to the hub plane, to balance the tail rotor thrust, and the lateral cyclic pitch input θ_{1c} reduced significantly. For the UH-60, however, a roll-right auxiliary moment appeared to be optimal for vibration reduction. This moment produced a rightward shaft tilt and increased the lateral cyclic flapping to tilt the tip path plane substantially left relative to the hub plane (required to balance the tail rotor thrust). Consequently, a larger lateral cyclic pitch input was required. This optimal solution was nonintuitive, and bears testimony to the complex and highly coupled behavior of a helicopter rotor.

It was verified that reductions in vibration would indeed be obtained when the horizontal tail was actually used to generate the auxiliary pitching and rolling moments for the UH-60-type aircraft (rather than simple introduction of the auxiliary moments in the trim equations, without specification of its source). The collective and differential horizontal tail pitch inputs that minimized vibrations indeed produced a nose down and a roll-right moment, as expected. However, the rolling moment produced was relatively small, due to one-half of the horizontal tail being stalled. This suggests that a larger horizontal tail or an additional canard may be desirable if larger auxiliary moments are required.

References

[1]Reichert, G., "Helicopter Vibration Control–Survey," *Vertica*, Vol. 5, No. 1, 1981, pp. 1–20.

[2]Lowey, R. G., "Helicopter Vibrations: A Technological Perspective," *Journal of the American Helicopeter Society*, Vol. 29, No. 4, 1984, pp. 4–30.

[3]Friedmann, P. P., "Helicopter Vibration Rediction Using Structural Optimization with Aeroelastic/Multidisciplinary Contraints: A Survey," *Journal of Aircraft*, Vol. 28, No. 1, 1991, pp. 8–21.

[4]Friedmann, P. P., and Millott, T. A., "Vibration Reduction in Rotorcraft Using Active Control: A Comparison of Various Approaches," *Journal of Guidance, Control, and Dynamics*, Vol. 18, No. 4, 1995, pp. 664–673.

[5]Fradenburgh, E. A., and Chuga, G. M., "Flight Program of the NH-3A Research Helicopter," *Journal of the American Helicopter Society*, Vol. 13, No. 1, 1968, pp. 44–62.

[6]Arcidiacono, P. J., deSimone, G., and Occhiato, J., "Preliminary Evaluation of RASA Data Comparing Pure Helicopter, Auxiliary Propulsion and Compound Helicopter Flight Characteristics," *Journal of the American Helicopter Society*, Vol. 27, No. 1, 1982, pp. 42–51.

[7]Anderson, W. D., and Wood, E. R., "AH-56A (AMCS) Compound Helicopter Vibration Reduction," *Proceedings of the 30th Annual Forum of the American Helicopter Society*, American Helicopter Society, New York, 1974, Paper 834.

[8]Humpherson, D. V., "Compound Interest—A Dividend for the Future, Revised," 54th Annual Forum of the American Helicopter Society, Washington, DC, May 1998.

[9]Sekula, M., and Gandhi, F., "Evaluation of Helicopter Vibration Reductions and Changes in Trim Due to Auxiliary Lift and Propulsion," *Journal of Aircraft* (to be published).

[10]Stepniewski, W. Z., and Tarczynski, T., "Open Airscrew VTOL Concepts," NASA CR-177603, 1992.

[11]Bir, G., and Chopra, I., "University of Maryland Advanced Rotorcraft Code (UMARC) Theory Manual," Dept. of Aerospace Engineering, UM-AERO Rept. 92-02, Univ. of Maryland, College Park, MD, Aug. 1992.

[12]Howlett, J., "UH-60A Black Hawk Engineering Simulation Program: Volume I Mathematical Model," NASA CR-177542, USAAVSCOM TR 89-A-001, U.S. Army Aviation Systems Command, Sept. 1989.

A. Chattopadhyay
Associate Editor